Analytica Chimica Acta 651 (2009) 220–226

Contents lists available at ScienceDirect

Analytica Chimica Acta

journal homepage: www.elsevier.com/locate/aca

A novel cobalt hexacyanoferrate nanocomposite on CNT scaffold by seed medium and application for biosensor

Suiping Wang, Limin Lu, Minghui Yang, Yong Lei, Guoli Shen*, Ruqin Yu

State Key Laboratory for Chemo/Biosensing and Chemometrics, College of Chemistry and Chemical Engineering, Hunan University, Changsha 410082, PR China

ARTICLE INFO

Article history:
Received 12 May 2009
Received in revised form 31 August 2009
Accepted 2 September 2009
Available online 6 September 2009

Keywords:
Seed-mediated
Cobalt hexacyanoferrate nanoparticle
Carbon nanotube
Electrochemistry
Biosensor

ABSTRACT

In this paper, for the first time, we introduced the seed-mediated method to the growth of cobalt hexacyanoferrate nanoparticles (CoNPs), using 3.5 nm gold nanoparticles as seeds and multiwalled carbon nanotubes (MWCNTs) as growth scaffold which would both show synergistic action toward the reduction of H_2O_2. Via gold seeds, the one-step fabrication of CoNPs on the glassy carbon electrode is simple without any linking reagents, which will ingeniously exert the electrochemical properties of cobalt hexacyanoferrate. Combined with glucose oxidase, the sensing surface is applied as a biosensor for glucose. The growth of CoNPs is a chemical deposition process around the small Au nanoseed particles. The nanoseeds bridge the CoNPs and CNTs to form a smart nanocomposite. Spherical CoNPs have a relatively moderate dispersion on the three-dimensional network of CNTs with relatively even diameter ca. 100 nm. Whereas, in the control experiments without gold seeds cobalt hexacyanoferrate can only form continuous films, of which the size is far from nanolevel and the catalytic ability is poor. The synthesis and fabrication/modification of CoNPs are simple and fast without prior preparation of CoNPs and lengthy process of cross-linking. The amount of the seeds and CNTs, growth time and concentration of growth solution were investigated. Scanning electron microscopy (SEM) and electrochemical method were used.

1. Introduction

Nanostructure materials are very attractive due to their unique optical, electrical, catalytic and magnetic properties and have found potential applications in nanoelectronic devices, nanosensors and catalysts [1–5]. Single-component nanomaterials, such as metals, metal oxides, polynuclear transition metal cyanides, sulfides, silicon dioxide and polymers have been greatly focused for the past decades. While composite nanomaterials show predominance of the merit or virtue integration of individual components, called as synergistic effect and functionality, which would greatly improve the performance of biosensors. The synergy is usually realized by simple entrapment or encapsulation of the individual components to get enhanced signal [6–8]; the case of bifunctional or multifunctional nanomaterials is more diverse and complex [9–11].

Carbon nanotubes (CNTs) consist of graphitic sheets, which have been rolled up into a cylindrical shape. Due to the unique electrical properties, high chemical stability and high surface-to-volume ratio, CNTs have been intensively researched for electrocatalytic and sensing applications [12]. Multiwalled carbon nanotubes (MWCNTs) usually have 2–100 nm diameter (typically 2–10 nm internal diameter) while the single layer cylindrical graphite sheet of single-walled carbon nanotubes (SWCNTs) are usually about 0.2–2 nm in diameter. The length of the CNTs can vary from micrometers to centimeters with a very high aspect ratio, which would be a good scaffold for composite nanomaterials [13].

Metal hexacyanoferrates (MHCFs), an important class of mixed-valence compounds, have attractive electrocatalytic, electrochromic, ion-exchanging, ion-sensing, and photomagnetic properties. As a group of excellent electron-transfer mediators these inorganic polymers have been widely used in electrochemistry to electrocatalyze the oxidation of guanine, DNA, deoxyguanosine, dopamine, ascorbic acid, NADH, glutathione, cysteine and H_2O_2 [14–20] and the reduction of Fe^{3+}, CO_2 and hydrazine [21–23]. Among the hexacyanoferrates, cobalt hexacyanoferrate (CoHCF) would be especially attractive because of its interesting chemical and electrochemical properties [24–27]. It exhibits excellent reversible redox centers very similar to those of Prussian blue while its electrochemical activity affected by electrolyte cation behaves differently from Prussian blue [28,29]. The traditional methods to prepare MHCFs include chemical deposition [30], electrochemical deposition [31], Langmuir–Blodgett technique [32] and reversed micelle synthesis [33]. The modification of MHCFs on substrates involves mechanical rub, electrodeposition, self-assembly and entrapment or encapsulation [30,31,34]. However, the preparation of nanoMHCFs and their modification on substrates are usually performed step-by-step. It is a challenge to control over the morphology and the size of MHCFs or to cre-

* Corresponding author. Tel.: +86 731 8821355; fax: +86 731 8821355.
E-mail address: glshen@hnu.cn (G. Shen).

0003-2670/$ – see front matter © 2009 Published by Elsevier B.V.
doi:10.1016/j.aca.2009.09.004

ate advanced and functional building blocks for the development of innovative nanomaterials and smart nanodevices.

To our best knowledge, few researches of nanoMHCFs composite have been carried out. For instance, Kumar et al. reported a one-step electrochemical deposition of gold-Prussian blue nanocomposite films in which each phase can control the growth of the other [35]; Cheng et al. devised a site-selective self-assembly of 3-mercaptopropionic acid-bridged CuHCF multilayers on (3-aminopropyl) trimethoxysilane-supported gold colloid [36]; Qiu et al. synthesized Prussian blue shell/Au core hybrid composite in solution and used layer-by-layer technique to fabricate on ITO glass through polyelectrolyte [37].

Oyama's research group reported a series of work on metal nanoparticle-attached indium tin oxide surface by seed-mediated growth, where metal nanoparticles ca. 60 nm have been grown firmly around small size seed particles by alternately immersing into seed solution and growth solution [38–40]. Briefly, the nanoseed particles are attached on the ITO surface by just immersing into relevant seed solution containing metal nanoparticles of ca. 4 nm. The crystal growth of metal nanoparticles on the ITO surface is possible when immersing the nanoseed-attached substrate into the growth solution, which contained metal ions, cetyltrimethylammonium bromide (CTAB) and ascorbic acid as reductant. Seed-mediated growth is used to prepare nanomaterials in solution, especially for metal nanostructure. However, its application to fabricate biotransducer is scarce.

Our research was aimed at the seed-mediated method for fabricating cobalt hexacyanoferrate nanoparticles (CoNPs) on CNTs modified glassy carbon electrode (GC). The approach is quite simple because the growth of CoNPs was completed in one step, i.e., only by immersing into the growth solution. This electrochemical function nanomaterial (without using any peculiar binder molecules or entrapment reagents) can sufficiently contact the detection target, exhibiting high electron-transfer ability and attractive electrocatalytic properties. Combined with glucose oxidase, the sensing surface is applied as a biosensor for glucose.

2. Experimental

2.1. Reagents and apparatus

MWNTs with approximately 95% purity were obtained from Shenzhen Nanotech Port Co. Ltd. (Shenzhen, China). Chloroauric acid ($HAuCl_4{\cdot}3H_2O$), trisodium citrate and sodium borohydride ($NaBH_4$) were all purchased from Sinopharm Chemical Reagent Co. Ltd. (Shanghai, China). Glucose oxidase (GOx, from Aspergillus niger; EC 1.1.3.4, type VII-S; 196,000 unit g^{-1}) was purchased from Sigma. KCl, $CoCl_2$, $K_3Fe(CN)_6$ and any other reagents were of analytical grade. Ultra pure water was used throughout with a resistance of 18.2 MΩ cm.

Scanning electron microscopy (SEM) analysis was performed using a JSM-5600LV microscope (JEOL Ltd., Japan). Cyclic voltammetric and amperometric measurements were carried out on CHI 760B electrochemical workstation (Shanghai, China). A three-electrode cell (10 mL) was used with the modified glassy carbon electrode (GC) as the working electrode, a saturated calomel electrode (SCE) as reference electrode and a platinum foil electrode as counter electrode. All potentials were measured and reported versus the SCE and all experiments were carried out at room temperature.

2.2. Preparation of gold seeds

The 3.5 nm Au nanoparticles (AuNPs) were synthesized by the method reported previously [41]. Briefly, 0.6 mL of ice cold 0.1 M $NaBH_4$ was added to 20 mL aqueous solution containing 2.5×10^{-4} M $HAuCl_4$ and 2.5×10^{-4} M trisodium citrate under stirring. The solution immediately turned orange-red, indicating the formation of 3.5 nm gold nanoparticles, denoted as Au(seed) in the context. Prior to any further experimentation, the seed particles were stored at 25 °C for 3 h to allow excess borohydride to be decomposed by water. The Au(seed) is stable for a couple of weeks stored at 4 °C. The average size measured from transmission electron microscopy was 3.5 ± 0.7 nm.

2.3. Treatment of carbon nanotubes

The CNTs were purified as reported previously [6]. Briefly, 100 mg of CNT was oxidized at 400 °C for 30 min to remove amorphous carbon particles. Then, the oxidized carbon nanotubes were dispersed in 60 mL of 6.0 M HCl for 4 h under ultrasonic agitation eliminating metal oxide catalyst. Finally, they were washed until the pH of the solution was neutral and dried for further use. The CNTs were dispersed in ethanol by ultrasonic bath with a concentration of 2 mg mL^{-1}.

2.4. Fabrication of the electrodes

Glassy carbon electrodes (4-mm diameter) were polished with emery paper and alumina slurry consecutively, then cleaned under bath sonication alternatively with water and ethanol and finally thoroughly rinsed with distilled water.

Typical procedures to attach CoNPs on CNTs modified electrode adopted eventually in this work are as follows: 10 μL solution of CNT was first cast on the GC surface laying in room temperature for the evaporation of ethanol (step 1). Next 10 μL Au(seed) solution was dropped on the thin film of CNTs (step 2). After drying, the electrode was immersed into the fresh prepared growth solution containing 0.25 M KCl, 0.5 mM $CoCl_2$ and 0.25 mM $K_3Fe(CN)_6$ for 2 h for the growth of CoNPs (step 3). The modified electrode was denoted as CoNP/Au(seed)/CNT/GC, other electrodes such as Au(seed)/CNT/GC, CoNP/Au(seed)/GC were prepared in a similar manner.

2.5. Enzyme immobilization

Equal volumes of 20 mg mL^{-1} GOx, 1% BSA and 2.5% glutaric dialdehyde were mixed and 10 μL of the mixture was cast onto the surface of CoNP/Au(seed)/CNT/GC and dried at 4 °C in a refrigerator.

3. Results and discussion

3.1. Morphology of the CoNP/Au(seed)/CNT

The modified GC as prepared in Section 2.4, was characterized by scanning electron microscope. Fig. 1 shows a series of the typical SEM micro morphologies of the relevant modified GC surface. The modified GC of Fig. 1A is performed by Section 2.4 step 3; Fig. 1B is step 1 plus step 3; Fig. 1C is step 1 plus step 2; and Fig. 1D is step 1 plus step 2 and 3. It can be seen from Fig. 1A, *in situ* chemical deposition CoHCF stretched into continuous agglomerated film whose size is far from the nanolevel and so in the case in Fig. 1B the film of CoHCF covers densely over the CNTs which are totally buried and the electrochemical properties of which might be considerably blocked, compared with CNT/Au(seed)/CoNP (Fig. 1D). In Fig. 1C, the CNTs spread and twist while gold seeds are difficult to recognize due to the resolution of the SEM. With the introduction of gold seeds, Fig. 1D presents a distinct contrast to the CoHCF films of Fig. 1A and B. Spherical CoNPs have a relatively moderate dispersion on the Au(seed) attached CNTs, which confirms that the CoNPs grow well on the CNTs with the aid of the AuNP seeds. Gold

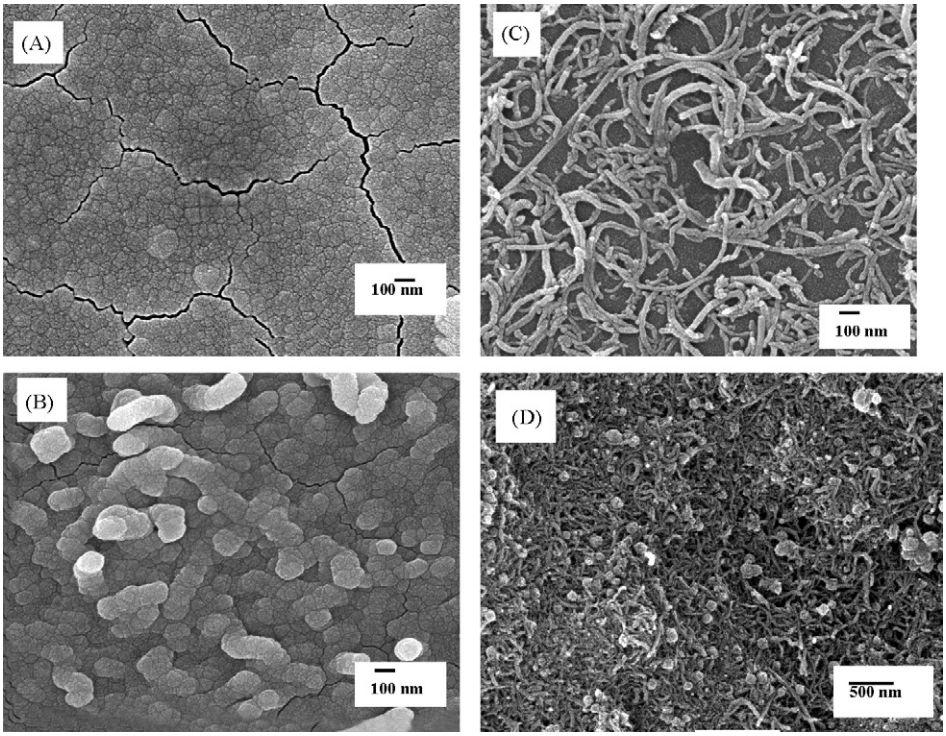

Fig. 1. Typical SEM images of the relevant modified GC surface: (A) CoHCF film, (B) CNT/CoHCF film, (C) CNT/Au(seed), and (D) CNT/Au(seed)/CoNP.

nanoseeds can physically adsorb onto substrate of normal glass [39]. Herein, the CNTs wind and twist spatially with large surface area which would be benefit to enhance physisorption between the CNTs and the gold seeds. The growth of CoNPs is a chemical deposition process around the small Au nanoseeds, which is known as a precursor method in the filed of catalysis [42]. In general, the small size gold seeds act as nucleation sites in the seed-mediated growth method; but the exact mechanism of the initial nucleation, growth and shape control is yet not clear. We presume that the negative citrate protected AuNP could attract positive Co^{2+} cations by electrostatic adsorption, which would assist cobalt hexacyanoferrate to deposit around the Au seed. From the SEM image we can see that the CNTs provide a net-like support to CoNP/Au(seed), which appears a fluffy and rough net bearing the CoNPs growing around the attached gold seeds. The size of the CoNPs is relatively uniform with the diameter ca. 100 nm and the distribution is relatively even with few clumps sticking from individual CoNPs on the upper surface of the CNTs net. Due to the enwinding three-dimensional network of the CNTs, the CoNPs grow transversely and longitudinally within this stereo net. The as-prepared nanostructure will bring sufficient exposure to the electrochemical reactant, which would be very useful to exert its electrochemical and electrocatalytic properties. Meanwhile, the enwrapped gold nanoseeds in CoNPs would also be helpful to electron transfer. Further eletrochemical experiments were carried out for demonstration in the following section.

3.2. Electrochemical characterization of the seed-mediated CoNPs composite electrode

Fig. 2 illustrates the typical cyclic voltammograms (CVs) of the CoNP/Au(seed)/CNT/GC obtained in 0.5 M KCl, 0.5 M NaCl and 0.1 M NaH_2PO_4 at the scan rate of 20 mV s^{-1}. It can be seen that the CV shape (number and position of the redox peaks) depends on the type of the supporting electrolyte. In NaCl solution (curve A), two pairs of redox peaks can be observed and the formal potentials ($E^\circ = [(E_{p,a} + E_{p,c})/2]$) are 0.40 and 0.85 V, respectively. The two pairs of redox peaks were explained as the existence of two stoichiometries of CoHCF, $Na_2Co^{II}[Fe^{II}(CN)_6]$ and $NaCo_{1.5}{}^{II}[Fe^{II}(CN)_6]$ [43]. The peaks at 0.40 and 0.85 V are attributed to transformation between Fe(II) and Fe(III) in the redox couples of $Co_{1.5}{}^{II}Fe^{III}(CN)_6/NaCo_{1.5}{}^{II}Fe^{II}(CN)_6$ and $NaCo^{II}Fe^{III}(CN)_6/Na_2Co^{II}Fe^{II}(CN)_6$, respectively. According to the previous reports [14,43,44], the redox reactions with the involvement of Na^+ can be expressed as follows:

$$Co_{1.5}{}^{II}Fe^{III}(CN)_6 + e^- + Na^+ \rightleftharpoons NaCo_{1.5}{}^{II}Fe^{II}(CN)_6 \quad (1)$$

$$NaCo^{II}Fe^{III}(CN)_6 + e^- + Na^+ \rightleftharpoons Na_2Co^{II}Fe^{II}(CN)_6 \quad (2)$$

The number of redox peaks and the peak potential in NaH_2PO_4 (curve C) is almost same as that in NaCl. However, the two anodic peaks merged into one in KCl solution (curve B); a pair of well-defined redox peaks near 0.50 V and another obvious cathodic peak near 0.65 V can be observed.

Fig. 3 shows the CVs of the CoNP/Au(seed)/CNT modified electrode in 10 mM phosphate-buffered saline (PBS) containing 0.1 M KCl at different scan rates. As can be seen, both the anodic and the catholic peak currents increase with increasing potential scan rates. The inset line plots are the square root of the scan rates versus current responses, indicating the diffusion-controlled process of the modified electrode.

Cyclic voltammetry is a powerful tool for investigating the properties of the modified interface. Fig. 4A shows the CVs of the CoNP/Au(seed)/CNT electrodes with different volume of Au(seed) solution (a) 0 μL; (b) 10 μL; (c) 20 μL in 0.1 M NaH_2PO_4. CNTs commonly do not affect the electron-transfer process between the redox polymer film and the electrode support without virtual change in the shape or peak potentials of the CV [8]. In Fig. 4A curve b, there are two sets of distinct redox peaks with the formal potentials ($E^\circ = [(E_{p,a} + E_{p,c})/2]$) of about 0.41 and 0.86 V, which attribute to the characteristic electrochemistry of cobalt hexacyanoferrate [14]. The wave around 0.2 V is thought to be the CNTs' background

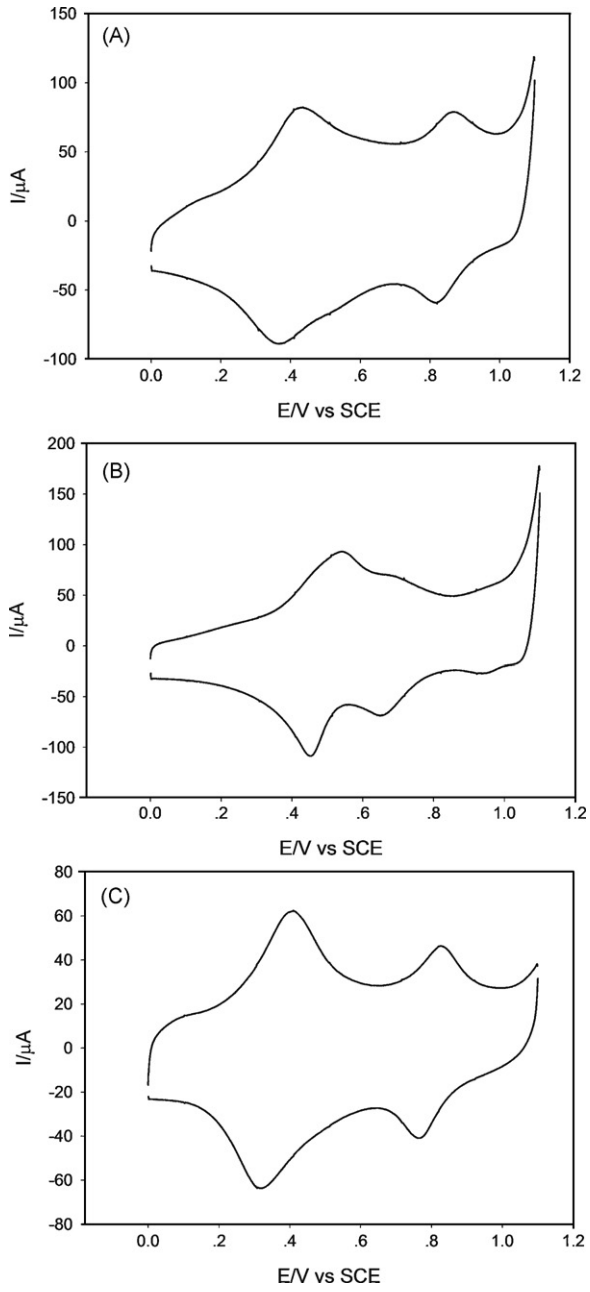

Fig. 2. CVs of the CoNP/Au(seed)/CNT electrodes in 0.5 M NaCl (A), 0.5 M KCl (B), and 0.1 M NaH_2PO_4 (C) at the scan rate of 20 mV s^{-1}.

which is not overwhelmed by the peak of CoNPs. The characteristic rodox peaks of cobalt hexacyanoferrate can be also identified in Fig. 4A cure c. The current signal of curve a (without Au seeds) has much weaker of that characteristic redox peaks compared with that of curve b and c (with Au seeds) in Fig. 4A. From Fig. 4A, we can even see that the current responses with Au(seed) are larger than that without Au(seed), suggesting the growth of CoNPs under the existence of Au(seed) was beneficial to the electrochemical response. This is well consistent with the scanning electron micrograms, that is, the electrochemical response of CoNPs is much larger than that of CoHCF film, supporting the seed mediated growth of CoNPs. However, the current signal of curve b (10 μL seed solution) is much larger than that of curve c (20 μL seed solution), not as initially anticipated. The reason might be that gold seeds compete for reacting species and too much gold seeds are not good for growing CoNPs of uniform size, shape and dispersion

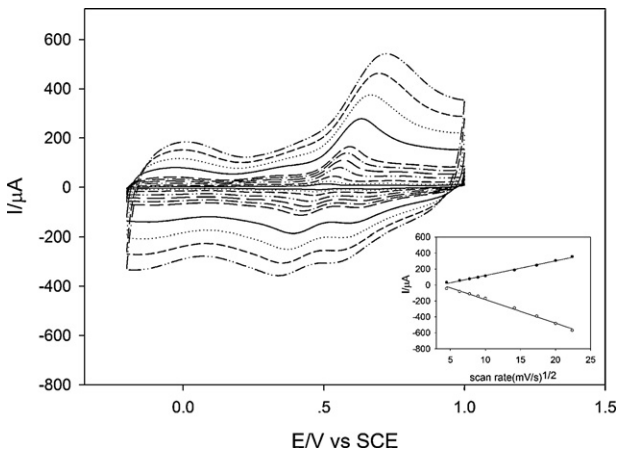

Fig. 3. CVs of the CoNP/Au(seed)/CNT modified electrode in 10 mM PBS (pH 7.0) containing 0.1 M KCl at different scan rates (from inner to outer): 0.005, 0.01, 0.02, 0.04, 0.06, 0.08, 0.1,0.2, 0.3, 0.4, and 0.5 V s^{-1}.

which relates tightly to its electrochemical and electrocatalytic properties.

According to the enhanced current signals in Fig. 4A, the advantages of the CoNP/Au(seed)/CNT nanocomposite were further illustrated in connection with the detection of hydrogen peroxide. Fig. 4B shows the amperomeric responses for successive addition of 1 mM H_2O_2 of the CoNP/Au(seed)/CNT electrodes

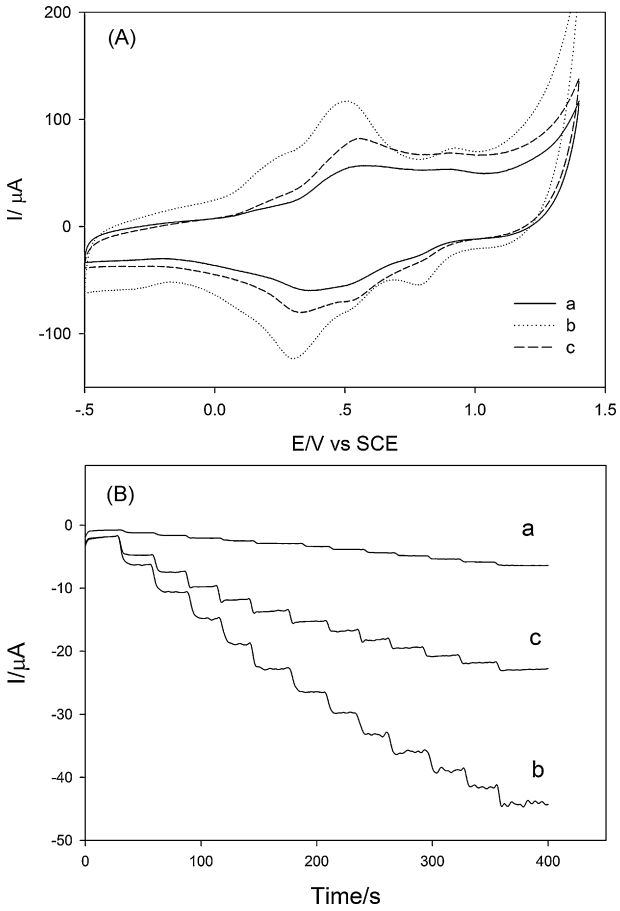

Fig. 4. (A) CVs of the CoNP/Au(seed)/CNT electrodes with different volume of Au(seed) solution (a) 0 μL; (b) 10 μL; (c) 20 μL in 0.1 M NaH_2PO_4. Scan rate, 50 mV s^{-1}. (B) Current–time recordings of the CoNP/Au(seed)/CNT electrodes with different volume of Au(seed) solution (a) 0 μL; (b) 10 μL; (c) 20 μL for successive addition of 1 mM H_2O_2 in 0.1 M NaH_2PO_4 at −0.1 V.

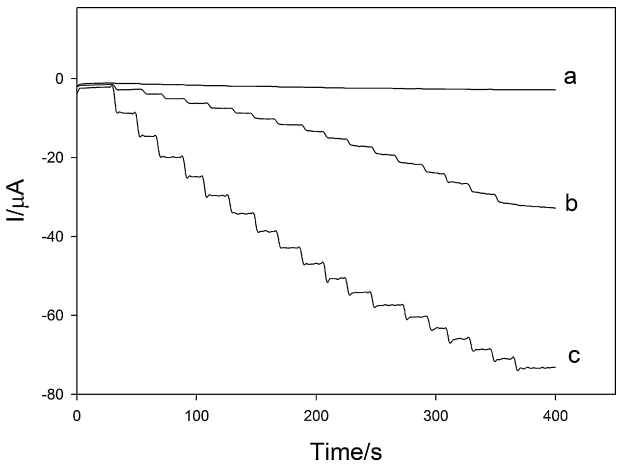

Fig. 5. Current–time curves of 1 mM H_2O_2 at CoNP/Au(seed) (a), Au(seed)/CNT (b) and CoNP/Au(seed)/CNT (c) electrodes in 0.1 M NaH_2PO_4 at −0.1 V.

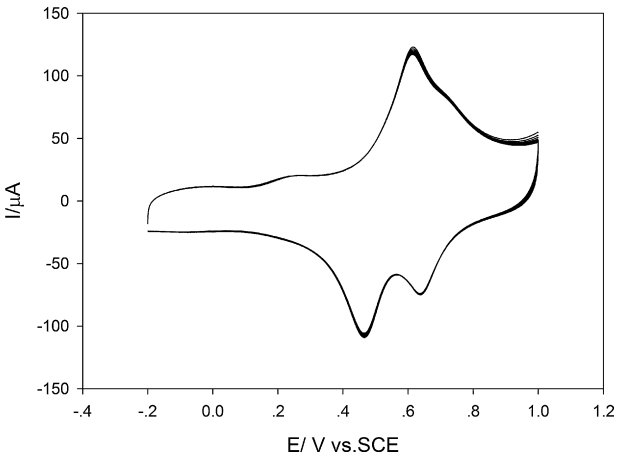

Fig. 6. Consecutive 10 CV cycles of the glucose biosensor in 10 mM PBS (pH 7.0) containing 0.1 M KCl at 50 mV s^{-1}.

with different volume of Au(seed) solution (a) 0 μL; (b) 10 μL; (c) 20 μL at the potential of −0.1 V. The responses with Au seed (CoNP/Au(seed)/CNT) are much larger than that without Au seed (CoNP/CNT) and the electrode with 10 μL seed solution has the largest current signal which quite agrees with the CVs of Fig. 4A. The linear range of the modified electrode with 0, 10, and 20 μL Au(seed) solution toward H_2O_2 is 1×10^{-5} to 8×10^{-3}, 8×10^{-7} to 1.2×10^{-2}, 5×10^{-6} to 1×10^{-2} M with the sensitivity of 3.57, 39.8 and 18.65 μA mM^{-1} cm^{-2}, respectively. The seed-mediated growth of CoNPs catalyzes the reduction of hydrogen peroxide, improving greatly the electrochemical response. Repeated use of the CoNP/Au(seed)/CNT/GC did not affect the repeatability and the long term stability. For instance, 1 mM H_2O_2 was measured continuously for 6 times, and a relative standard deviation (RSD) of 4.1% was obtained.

In order to discern the role of the individual components and possible synergy between them, amperometry was performed for the step modified GC. Fig. 5 displays the current–time curves of the CoNP/Au(seed) (a), Au(seed)/CNT (b) and CoNP/Au(seed)/CNT (c) electrodes for the detection of 1 mM H_2O_2 at the potential of −0.1 V. The CoNP/Au(seed)/CNT modified electrode shows the largest and most rapid response which exhibits one main advantage of the electrocatalytic properties of CoNPs capable to catalyze the reduction of H_2O_2 at low potential and prevent interference from other electroactive substances. In particular, the current response of the CoNP/Au(seed)/CNT electrode (c) was about 36.5 times that of the CoNP/Au(seed) (a) and 4.7 times that of the Au(seed)/CNT (b). It is worth noting that the current response of the CoNP/Au(seed)/CNT electrode is much larger than that of the summation of the other two electrodes. The improvement could be ascribed to the synergistic action between the CoNPs and CNTs, which leads to the enhanced redox activity of CoNPs. The introduction of CNTs facilitates the electroreduction of H_2O_2 (by CoNPs) for its inherent fast electron-transfer property; another important aspect is the enwrapped gold nanoseeds in the CoNPs would also be helpful to electron transfer; herein, both promotions were attributed to synergistic action.

To get a preferable electrochemical performance of this sensing surface, growth time was carefully studied. The electrocatalytic response increases with the increasing growth time and gets to the peak at 2 h, which may be ascribed to the size-dependent effect of the CoNPs. The adopted concentration of growth solution in this paper had also been optimized. The electrochemical response increased with increasing amount of CNTs, while too much amount of CNTs will decrease the stability of the sensing surface. 10 μL CNT (2 mg mL^{-1}) was chosen for the experiment to get a stable and content response. Supporting electrolytes were investigated by the electrochemical response of cyclic voltammetry and amperometry to H_2O_2. The largest electrochemical response has been figured out in 0.1 M NaH_2PO_4 after experimented in 0.1 M NaCl, 0.1 M KCl, 10 mM PBS (pH 7.0) and 10 mM PBS (pH 7.0)/0.1 M KCl. Ionic strength and ion types were not taken into account, the solution of 0.1 M NaH_2PO_4 is acidic which is quite agreeable with the general opinion that the redox activities of MHCFs prefer in acid media [45].

3.3. Performance of the glucose biosensor

The excellent electrocatalytic activity toward H_2O_2 means a new platform for fabricating oxidase based electrochemical biosensors. Here, glucose oxidase was selected as a model enzyme and immobilized onto the CoNP/Au(seed)/CNT electrode by cross-linking of glutaric diadehyde. Experiments were performed in the phosphate buffer solution, which is commonly used for glucose biosensor.

The stability of the biosensor was investigated by successive CVs in the PBS over potential range from −0.2 to 1.0 V at the scan rate of 50 mV s^{-1}. As shown in Fig. 6, the electrochemical interface is fairly stable without significant current change during the consecutive 10 CV cycles.

The working potentials between −0.3 V and +0.4 V were investigated. There are very weak reductive signals or hardly any signals over the potential range except that distinct reductive current appears at −0.1 V. Common redox-active substances in physiological sample are interference-free in such low working potential as −0.1 V [46]. Fig. 7 shows the typical current–time curve for the biosensor upon the injection of glucose and electroactive interferences. Compared with the current response of 0.5 mM glucose (Glu), the responses generated by 0.1 mM ascorbic acid (AA) and uric acid (UA) were essentially negligible, which demonstrates the good selectivity. The low detection potential makes it attractive for electrochemical biosensor.

Fig. 8 shows the amperometric response at the CoNP/Au(seed)/CNT modified biosensor toward successive addition of 0.5 mM glucose in 10 mM PBS (pH 7.0) containing 0.1 M KCl at the potential of −0.1 V. Stable, repeated and fast responses were observed with steady state reached within 10 s. The liner range is from 0.005 to 2 mM with the detection limit of 0.5 μM (3 *S*/*N*). The repeatability of the biosensor was investigated by continuous measurement to 0.25 mM glucose for 10 times and a RSD of 3.1% was obtained, which implies good repeatability for practical application. The reproducibility of the biosensor was also

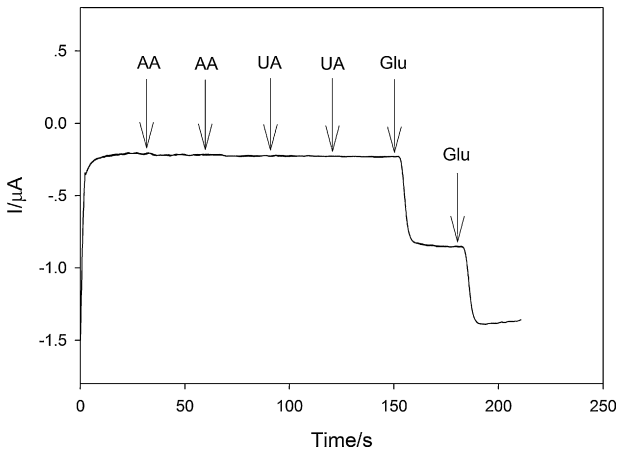

Fig. 7. Amperometric responses of the glucose biosensor to the successive additions of 0.1 mM AA, UA and 0.5 mM glucose in 10 mM PBS (pH 7.0) containing 0.1 M KCl at −0.1 V.

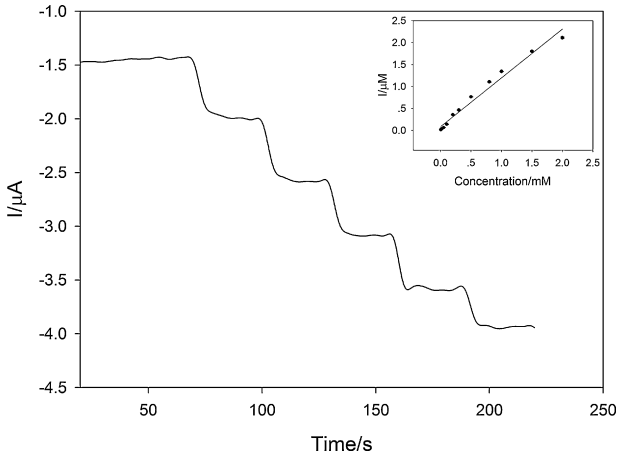

Fig. 8. Amperometric response of CNT/Au(seed)/CoNP-GOx electrode to subsequent additions of 0.5 mM glucose in 10 mM PBS (pH 7.0) containing 0.1 M KCl at −0.1 V. The inset is the calibration curve with the error bars of the standard deviation for three repeated measurements.

tested by six biosensors and a RSD of 4.6% was obtained toward 0.25 mM glucose, indicating the reliability of the method.

As a preliminary evaluation of the validity of the proposed electrochemical biosensor, the recovery of glucose with different concentration in spiked urine samples from a healthy volunteer was testified as shown in Table 1. The recovery is from 98.7 to 104% which reveals that the newly proposed biosensor could be used in practical applications.

The method of as-prepared biosensor based on seed medium is quite different from the traditional chemical and electrochemical method for biosensors based on MHCFs. The performance of the present glucose biosensor is comparable with the previous MHCFs based glucose biosensor. For instance, the performance of the linear range and the detection limit is better than that reported for the glucose biosensor based on electrodeposition of CoHCF [47], and based on layer-by-layer membranes of polyamidoamine stabilized gold nanoparticles and poly(vinylsulfonate) which were covered by electrochemically deposited CoHCF [48], and based on adsorbed Prussian blue (prepared by chemical method in advance) solid carbon paste [49], and based on palladium hexacyanoferrate hydrogel/electrodeposited nickel hexacyanoferrate [50], and based on alternately electrodepositing hybrid polypyrrole/copper hexacyanoferrate [51].

Table 1
Analysis of spiked urine samples by the biosensor ($n = 3$).

Added (mM)	Found (mM)	Recovery (%)	RSD (%)
0.05	0.052	104	4.67
0.20	0.198	99.0	2.35
1.00	0.987	98.7	1.20

The one-step preparation and attachment of CoNPs is a rather simple method, i.e., *in situ* chemical deposition in growth solution mediated by Au seeds. Without any binding reagents, exposed nanoscale material with large surface area could directly touch the electrochemical active substance and lead to improved response. The gold nanoparticle, as a juncture, bridges the CoNPs and CNTs to form a smart nanocomposite. The seed-mediated growth method improves significantly the performance of the sensing through ingenious combination of the individual nanomaterials. The present composite style for CoNPs is different from previous reports of encapsulation, self-assembly and layer-by-layer techniques. One obvious advantage is that synthesis and fabrication are simultaneous which is fairly simple and fast. Another important advantage is that without couple reagent it would be better to exert the inherent electrocatalytic properties of CoNPs reinforced with CNTs ingeniously.

4. Conclusions

A novel method of compositing nanomaterial for CoNPs with a single step preparation and fabrication has been worked out by seed medium. The CoNP nanocomposite synergized by CNTs has excellent selectivity and electrocatalytic ability. Via gold seeds, the one-step synthesis/fabrication of CoNPs on the substrate is simple without any couple reagents. This strategy could be extrapolated to obtain other homo- and hetero- MHCFs nanometer systems and could have a considerable amount of research space for composite nanomaterials.

Acknowledgements

This work was supported by the “973” National Basic Research Program of China (No. 2007 CB 310500) and the National Natural Science Foundation of China (Grants 90817101, 20775023).

References

[1] H. Chen, J. He, C. Zhang, H. He, J. Phys. Chem. C 111 (2007) 18033.
[2] F. Cheng, J. Zhao, W. Song, C. Li, H. Ma, J. Chen, P. Shen, Inorg. Chem. 45 (2006) 2038.
[3] T. Murakami, K. Ajima, J. Miyawaki, M. Yudasaka, S. Iijima, K. Shiba, Mol. Pharm. 1 (2004) 399.
[4] J.M. Kinsella, A. Ivanisevic, J. Am. Chem. Soc. 127 (2005) 3276.
[5] D.J. Maxwell, J.R. Taylor, S. Nie, J. Am. Chem. Soc. 124 (2002) 9606.
[6] F. Qu, M. Yang, G. Shen, R. Yu, Biosens. Bioelectron. 22 (2007) 1749.
[7] M. Zhang, W. Gorski, J. Am. Chem. Soc. 127 (2005) 2058.
[8] P.P. Joshi, S.A. Merchant, Y. Wang, D.W. Schmidtke, Anal. Chem. 77 (2005) 3183.
[9] A. Ambrosi, M.T. Castañeda, A.J. Killard, M.R. Smyth, S. Alegret, A. Merkoçi, Anal. Chem. 79 (2007) 5232.
[10] K. Ramanathan, M.A. Bangar, M. Yun, W. Chen, N.V. Myung, A. Mulchandani, J. Am. Chem. Soc. 127 (2005) 496.
[11] D. Tang, R. Yuan, Y. Chai, Anal. Chem. 80 (2008) 1582.
[12] D. Tasis, N. Tagmatarchis, A. Bianco, M. Prato, Chem. Rev. 106 (2006) 1105.
[13] X. Yu, B. Munge, V. Patel, G. Jensen, A. Bhirde, J.D. Gong, S.N. Kim, J. Gillespie, J.S. Gutkind, F. Papadimitrakopoulos, J.F. Rusling, J. Am. Chem. Soc. 128 (2006) 11199.
[14] S.M. Chen, M.F. Lu, K.C. Lin, J. Electroanal. Chem. 579 (2005) 163.
[15] T.R.L.C. Paixão, C.C.M. Garcia, M.H.G. Medeiros, M. Bertotti, Anal. Chem. 79 (2007) 5392.
[16] M. Jiang, X.Y. Zhou, Z.F. Zhao, Ber. Bunsen-Ges. Phys. Chem. 95 (1991) 720.
[17] C.X. Cai, H.X. Ju, H.Y. Chen, Anal. Chim. Acta 310 (1995) 145.
[18] G.Y. Shi, J.X. Lu, F. Xu, W.L. Sun, L.T. Jin, K. Yamamoto, S.G. Tao, J.Y. Jin, Anal. Chim. Acta 391 (1999) 307.
[19] S. Zhang, W.L. Sun, W. Zhang, W.Y. Qi, L.T. Jin, K. Yamamoto, S.G. Tao, J.Y. Jin, Anal. Chim. Acta 386 (1999) 21.

[20] B.D. Humphrey, S.J. Sinha, A.B. Bocarsly, J. Phys. Chem. 91 (1987) 586.
[21] K. Ogura, M. Nakayama, C. Kusumoto, J. Electrochem. Soc. 143 (1996) 3606.
[22] D.R. Shankaran, S.S. Narayanan, Russ. J. Electrochem. 38 (2002) 987.
[23] S.M. Golabi, F. Noor-Mohammadi, J. Solid State Electrochem. 2 (1998) 30.
[24] S.M. Chen, Electrochim. Acta 43 (1998) 3359.
[25] A. Abbaspour, M.A. Mehrgardi, Anal. Chem. 76 (2004) 5690.
[26] C.X. Cai, K.H. Xue, S.M. Xu, J. Electroanal. Chem. 486 (2000) 111.
[27] W. Tao, D. Pan, Y. Liu, L. Nie, S. Yao, J. Electroanal. Chem. 572 (2004) 109.
[28] V.D. Ivanov, A.R. Alieva, Russ. J. Electrochem. 36 (2000) 852.
[29] J. Joseph, H. Gomathi, G.P. Rao, J. Electroanal. Chem. 304 (1991) 263.
[30] A. Widmann, H. Kahlert, I. Petrovic-Prelevic, H. Wulff, J.V. Yakhmi, N. Bagkar, F. Scholz, Inorg. Chem. 41 (2002) 5706.
[31] K.M. Jeerage, W.A. Steen, D.T. Schwartz, Chem. Mater. 14 (2002) 530.
[32] S. Choudhury, N. Bagkar, G.K. Dey, H. Subramanian, J.V. Yakhmi, Langmuir 18 (2002) 7409.
[33] M. Arai, M. Miyake, M. Yamada, J. Phys. Chem. C 112 (2008) 1953.
[34] S. Bharathi, M. Nogami, S. Ikeda, Langmuir 17 (2001) 7468.
[35] S.S. Kumar, J. Joseph, K.L. Phani, Chem. Mater. 19 (2007) 4722.
[36] W. Cheng, S. Dong, E. Wang, Chem. Mater. 15 (2003) 2495.
[37] J.D. Qiu, H.Z. Peng, R.P. Liang, J. Li, X.H. Xia, Langmuir 23 (2007) 2133.
[38] J. Zhang, M. Kambayashi, M. Oyama, Electrochem. Commun. 6 (2004) 683.
[39] G. Chang, J. Zhang, M. Oyama, K. Hirao, J. Phys. Chem. B 109 (2005) 1204.
[40] G. Chang, M. Oyama, K. Hirao, J. Phys. Chem. B 110 (2006) 20362.
[41] A. Gole, C.J. Murphy, Chem. Mater. 16 (2004) 3633.
[42] H. Bönnemann, G. Braun, W. Brijoux, R. Brinkmann, T.A. Schulze, K. Seevogel, K. Siepen, J. Organomet. Chem. 520 (1996) 143.
[43] P.J. Kulesza, S. Zamponi, M.A. Malik, M. Berrettoni, A. Wolkiewicz, R. Marassi, Electrochim. Acta 43 (1998) 919.
[44] Q. Tang, W. Xiong, L. Long, Anal. Lett. 40 (2007) 1610.
[45] L.D. Feng, J.M. Shen, X.H. Li, J.J. Zhu, J. Phys. Chem. C 112 (2008) 7617.
[46] W. Zhao, J.J. Xu, C.G. Shi, H.Y. Chen, Langmuir 21 (2005) 9630.
[47] M. Florescu, M. Barsan, R. Pauliukaite, C.M.A. Brett, Electroanalysis 19 (2007) 220.
[48] F.N. Crespilho, M.E. Ghica, C. Gouveia-Caridade, O.N. Oliveira Jr., C.M.A. Brett, Talanta 76 (2008) 922.
[49] D. Moscone, D. D'Ottavi, D. Compagnone, G. Palleschi, Anal. Chem. 73 (2001) 2529.
[50] D. Iveković, S. Milardovic, B.S. Grabaric, Biosens. Bioelectron. 20 (2004) 872.
[51] P.A. Fiorito, C.M.A. Brett, S.I. Córdoba de Torresi, Talanta 69 (2006) 403.